Metastable states in the narrow soliton regime of $Rb_2ZnCl_4:Mn^{2+}$ inferred from ESR measurements

A. Kassiba*
Laboratoire des Couches Minces, Faculté des Sciences, Université de Marrakech, Marrakech, Morocco

M. Pezeril
Laboratoire de Spectroscopie du Solide, Faculté des Sciences, Université du Maine, route de Laval, 72017 Le Mans CEDEX, France

P. Molinie
Institut de Physique et Chimie des Materiaux, Université de Nantes, 2 rue de la Houssinière 44072 Nantes CEDEX, France

J. C. Fayet
Laboratoire de Spectroscopie du Solide, Faculté des Sciences, Université du Maine, route de Laval, 72017 Le Mans CEDEX, France
(Received 17 January 1989)

We study the narrow soliton regime near $T_c = 195$ K in Rb_2ZnCl_4 with the help of the paramagnetic probe Mn^{2+} ($S=\frac{5}{2}$, $I=\frac{5}{2}$), which fits the Zn^{2+} crystal site nicely. Clearing the hyperfine interaction out of the EPR spectrum enables us to account for the spin-crystal-field interaction in terms of an amplitude modulation and of a soliton density. For a slow cooling or a slow heating of Bridgman samples previously subjected to thermal cyclings around T_c we observe several temperature ranges of about 5 K marked by a stationary soliton density. We conclude that metastable states pinned by defects are also responsible for a large hysteresis. Because our measurements are essentially local, we cannot discriminate between a chaotic and a long-range order of the solitons.

INTRODUCTION

$^{55}Mn^{2+}$ ($S=\frac{5}{2}$, $I=\frac{5}{2}$) substituted at low concentration for $^{67}Zn^{2+}$ in Rb_2ZnCl_4, allows the completion of a set of local measurements on the incommensurate phase of this crystal. Indeed, $^{67}Zn^{2+}$ has no nuclear spin, while $^{87}Rb^{+}$ ($I=\frac{3}{2}$) and $^{35,37}Cl^{-}$ ($I=\frac{3}{2}$) are well adapted for NMR and nuclear quadrupole resonance (NQR) investigations, respectively. Since $^{55}Mn^{2+}$ fits the host nicely, the sensitivity of ESR enables us to monitor the modulation of the local crystal field with the help of diluted and weakly perturbing impurities through the quadrupolar spin-lattice interaction, as is for $^{87}Rb^{+}$ NMR Ref. No. 1 and for $^{35,37}Cl^{-}$ NQR.[2]

Presently, we focus on the multisoliton regime near $T_c = 195$ K which has been the object of early qualitative observations by ESR spectroscopy.[3] As for the plane-wave regime near the normal-incommensurate phase transition at $T_i = 305$ K,[4] a preliminary cleaning of the hyperfine interaction is required to clear out the influence of the lattice modulation on the distribution of the local resonance fields. Otherwise, we follow nearly the same theoretical framework, as for NMR investigations,[1] and we assume that the soliton density which is deduced from the ESR line shapes is an essential characteristic of the multisoliton lattice.

It turns out that defect-induced metastable states can account for anomalous results obtained on a particular sample submitted to a particular thermal cycling around T_c.

I. THEORY

In an incommensurate phase, a spin probe located at site $\mathbf{r}$ is influenced by its own displacement and by the displacements of the neighboring atoms located at $\mathbf{r}_i$ from their positions in the underlying, high-symmetry normal phase $T > T_i$. The deformation of the surrounding can be represented by terms such as

$$u(\alpha,i) = A(T)e(\alpha,i)\cos[\Phi(\mathbf{r}) - \Phi(\alpha,i)], \quad \alpha = x,y,z \ .$$

$\Phi(\mathbf{r})$ and $A(T)$ represent the local phase and the amplitude of the modulation, respectively. $e(\alpha,i)$ and $\Phi(\alpha,i)$ represent, respectively, the components and the phase of $\mathbf{r} - \mathbf{r}_i$.

In Rb_2ZnCl_4, for the external magnetic field $\mathbf{H}$ directed along the modulation a axis ($\equiv[100]$) the space-group symmetry of the high-temperature phase is D_{2h}^{16} (*Pnma*), the symmetry of the displacement field implies that the local shift of the resonance lines $\Delta H(\Phi)$ is an even function of the atomic displacements.[4] A power-series expansion up to second order gives

$$\Delta H(\Phi) = A^2(T)\{h_2 + h_2'\cos 2[\Phi(\mathbf{r}) - \Phi_2]\} \ . \qquad (1)$$

Apart from a global shift, the line shape is influenced by $A^2(T)h_2'\cos 2(\Phi')$; $[\Phi' = \Phi(\mathbf{r}) - \Phi_2]$. The parameters h_2, h_2' and Φ_2 depend on the ESR transition which is considered.

Let us assume, for the sake of simplicity, that the local linewidth is mainly influenced by the fluctuations of a first-order Hamiltonian with the same phase as the second-order displacement:

$$\mathcal{H}(t)=A(T,t)\{O_2^m\}\cos\Phi' .$$

$\{O_2^m\}$ represents a linear combination of Stevens spin operators, $\{O_2^m\}=\sum_m d_2^m O_2^m$. Using the semiclassical analysis of the resonance linewidth[5] as used in our earlier work,[4,6] the local linewidth is driven by nonsecular effects, according to

$$L(\Phi')=L_0+L_1\cos^2(\Phi')+L_2\sin^2(\Phi') , \quad (2)$$

where L_1 and L_2 depend on the spectral densities of the fluctuations of the amplitude and the phase, on the matrix elements of $\{O_2^m\}$, and on the frequency measurement. L_0 takes into account the line broadening through mechanisms irrelevant to the lattice modulation.

The experimental ESR line shape is given by

$$F(H)=\int_0^{2\pi} f(\{H-[H_0+\Delta H(\Phi')]\}/L(\Phi'))P(\Phi')d\Phi' , \quad (3)$$

where f is a local line shape, H_0 the resonance field position above T_i, and $P(\Phi')$ is the probability distribution of Φ' over the crystal.

In the multisoliton regime, the phase Φ obeys a sine-Gordon equation and we obtain

$$P(\Phi)=\{\Delta(T)+\cos^2[n(\Phi-\Phi_0)]/2\}^{-1/2}$$

and

$$P(\Phi')=\{\Delta(T)+\cos^2[n(\Phi'-\Phi_0')]\tfrac{1}{2}\}^{-1/2} ,$$

$$(\Phi'=\Phi-\Phi_2,\quad \Phi_0'=\Phi_0-\Phi_2)$$

with $n=6$ for Rb_2ZnCl_4 and the parameter $\Delta(T)$ leads to the soliton density according to

$$N_s(T)=(\pi/2)[K(1+\Delta)^{-1/2}]^{-1}$$

where K represents the elliptic integral of the first kind.[1] Φ_0 represents the origin of the modulation in the nearly commensurate domains.

In this simple theoretical framework, a constant amplitude is assumed and the crystal is considered as a continuum medium. A more refined theory shows that amplitude solitons are coupled to phase solitons.[7] Whatever the shortcomings in the theory are, we consider that the parameters of the model, deduced from a computer reconstruction of the experimental spectra, give a relevant description of the multisoliton regime and of the structural phase change at T_c. Particularly, we shall assume below that the stability of the soliton density when T varies indicates a stability of the structural phase.

II. EXPERIMENTAL PROCEDURE AND RESULTS

Two Rb_2ZnCl_4:$^{55}Mn^{2+}$ samples cleaved from different Bridgmann batches have been studied. The chemical products used for both batches have the same origin. Apart from the $^{55}Mn^{2+}$ probes, neither the purity, the concentration of dislocations, nor the other extended defects in the samples were controlled. No pollution by other paramagnetic impurities was detected by ESR. A rather good crystalline quality was deduced from a visual examination through a microscope. Nevertheless, in such crystals the dielectric peaks near the lock-in transition which are observed in high-quality samples are smeared.[8]

Sample A was studied at EPR X band (10 GHz). Due to an overlap, at high magnetic field, between the lines $\mathcal{F}_1$: $(m_s=\frac{3}{2}\rightarrow\frac{5}{2})$ and $\mathcal{F}_1'$: $(m_s=\frac{1}{2}\rightarrow\frac{3}{2})$, only the behavior of the low-field lines corresponding to $\mathcal{E}_1$: $(m_s=-\frac{5}{2}\rightarrow-\frac{3}{2})$ could be investigated. During the cooling run, the temperature was lowered by jumps of 0.2 K. Between each variation, the temperature at the sensor being stabilized with an accuracy of 0.1 K, a delay of about 10 min permitted a stability of the ESR spectra to be obtained. About 30 records were taken in the temperature range 180–240 K. The same slow sequence of thermal variation was repeated in the heating run, the sample being initially cooled quickly and stabilized at $T=160$ K. It is worth noting that the sample A was previously submitted to several thermal cyclings around T_i and around T_c in order to define the experimental and the computer procedure. Particularly, close to T_c and for large temperature jumps, we have observed a long relaxation time of the sample according to previous results.[3]

On the other hand, sample B was freshly cleaved from a recently grown single crystal and was studied at the Q Band (34 GHz). Both $\mathcal{E}_1$: $(m_s=-\frac{5}{2}\rightarrow-\frac{3}{2})$ and $\mathcal{F}_1$: $(m_s=\frac{3}{2}\rightarrow\frac{5}{2})$ can be investigated. Similar thermal cyclings were realized, except for the amplitude of the thermal jumps, which was about 1 K, and for a poorer temperature stabilization $\Delta T=0.3$ K. The larger jumps are an essential difference between the two experiments.

The simulation of the experimental spectra was done with the help of a computation program based on the conjugate-gradient method.[9] The model parameters are varied automatically until an excellent agreement between the experimental spectra and the calculated ones is obtained. We summarize in the following the different steps used for the simulation.

First, for each line $(\mathcal{E}_1,\mathcal{F}_1)$ the $^{55}Mn^{2+}$ hyperfine structure does not exhibit any significant difference in the commensurate phases ($T>T_i$ and $T<T_c$). Particularly when H is directed along the modulation axis a, the three nonequivalent paramagnetic sites possess the same hyperfine splitting. This allows us to deconvolute the experimental lines (Fig. 1) in the incommensurate phase by a single hyperfine sextuplet which is determined experimentally for each transition. Thus the distribution of the local resonance fields, only due to the modulation of the crystal field, is cleared out (Fig. 1).

The multisoliton regime is marked by embryos of the three discrete lines observed below T_c in agreement with a tripling of the unit cell $a(T<T_c)=3a(T>T_i)$. The plane-wave regime near T_i gives only two edge singularities corresponding to $\Phi'=(0,\pi)$, $\{\pm\pi/2\}$.

Then, the deconvoluted experimental lines were fitted using the theoretical model of Sec. I. This is exemplified in Fig. 2(a) for the $\mathcal{E}_1$, transition at the X band. A persistent shoulder on the high-field side of the reconstructed curve could not be erased. The theoretical model can-

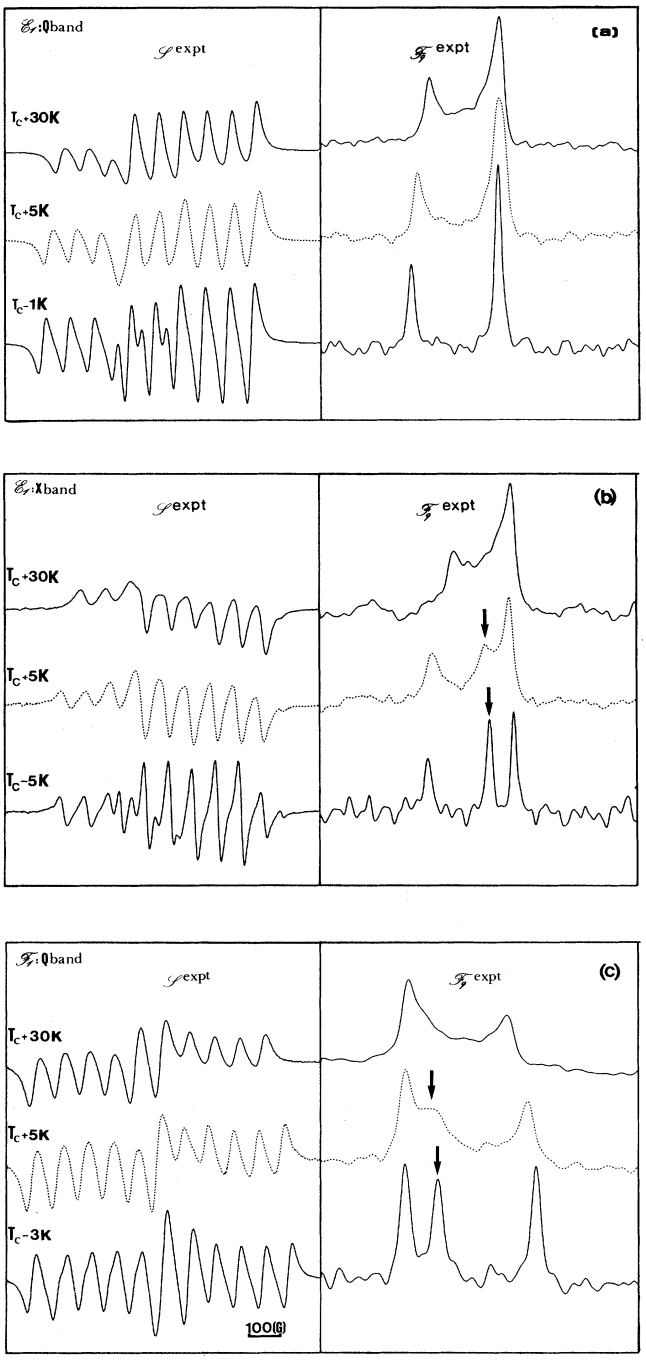

FIG. 1. Experimental EPR spectras $\mathcal{S}^{\text{expt}}$ and their corresponding quadrupolar local line-shift distributions $\mathcal{F}_q^{\text{expt}}$ obtained by a deconvolution of $\mathcal{S}^{\text{expt}}$ by the hyperfine sextuplet. (a) $\mathcal{C}_1(-\frac{3}{2}\rightarrow-\frac{5}{2})$ at Q band, (b) $\mathcal{C}_1$ at X band, (c) $\mathcal{T}_1(\frac{3}{2}\rightarrow\frac{5}{2})$ at Q band. Far from T_c (upper spectra a,b,c), we obtain two edge singularities according to a plane-wave regime. (a) Approaching T_c we obtain two sharp discrete lines with relative intensities 1 and 2. This is due to a particular value of $\Phi_0'\sim 30°$ (mod $\pi/3$). (b) and (c) The soliton regime (intermediate spectra) is marked by embryos (arrows) of the three discrete lines observed below T_c (lower spectra). The phases of Φ_0' are, respectively, 18.5° and 11° (mod $\pi/3$).

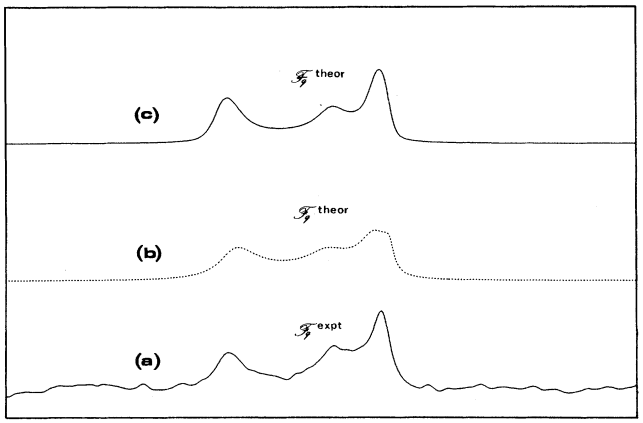

FIG. 2. Comparison between the experimental distribution (a) of the quadrupolar local line shift $\mathcal{F}_q^{\text{expt}}$ and the calculated ones (b) and (c) [Eq. (3)]. (b) Without an amplitude modulation. (c) With an amplitude modulation [Eq. (4)].

not account for the sharp edge singularity which is observed [Fig. 2(b)]. To overcome this discrepancy, we have allowed a modulation of the amplitude according to

$$A(T,\tau)=A_0(T)[1-\tau\cos(2\Phi')]\ . \tag{4}$$

Then, the reconstructed curve [Fig. 2(c)] reproduces nicely the features of the experimental one [Fig. 2(b)]. This adornment of the basic theoretical model, which is helpful in erasing a cumbersome edge singularity, can be supported by actual properties of the multisoliton lattice. Indeed, the amplitude-modulation term is equivalent to the introduction of high-order terms in the power-series expansion of $\Delta H(\Phi')$ [Eq. (1)]. Such terms may have a significant influence for a large amplitude of the atomic displacements, i.e., near T_c. On the other hand, the edge singularities $\Phi'=(0,\pi)$, $\{\pm\pi/2\}$ are reminiscent of the plane-wave regime and arise from probes inside discommensurations. They are submitted to large fluctuations, driven by the evolution of the underlying Goldstone mode[10] and to amplitude solitons coupled to phase solitons.[7] Briefly, the parameter τ has the virture of taking into account various mechanisms which act differently on the edge singularities arising from the discommensurations and on the sharp lines due to the commensurate domains.

Finally, the parameters of the improved phenomenlogical model derived from the theory were adjusted using a reverse procedure, i.e., a convolution by the hyperfine structure. Typical reconstructed spectra are compared to the experimental ones (Fig. 3). The soliton density derived from the fitted parameter $\Delta(T)$ is represented in Fig. 4. Below T_c, the fit of the experimental lines with the soliton model yields a smooth variation of $N_s(T)$ from 0.3 to 0.18 over a temperature range of about 5 K.

At lower temperature, i.e., below T_c-5 K, we were unable to discriminate between a residual density of

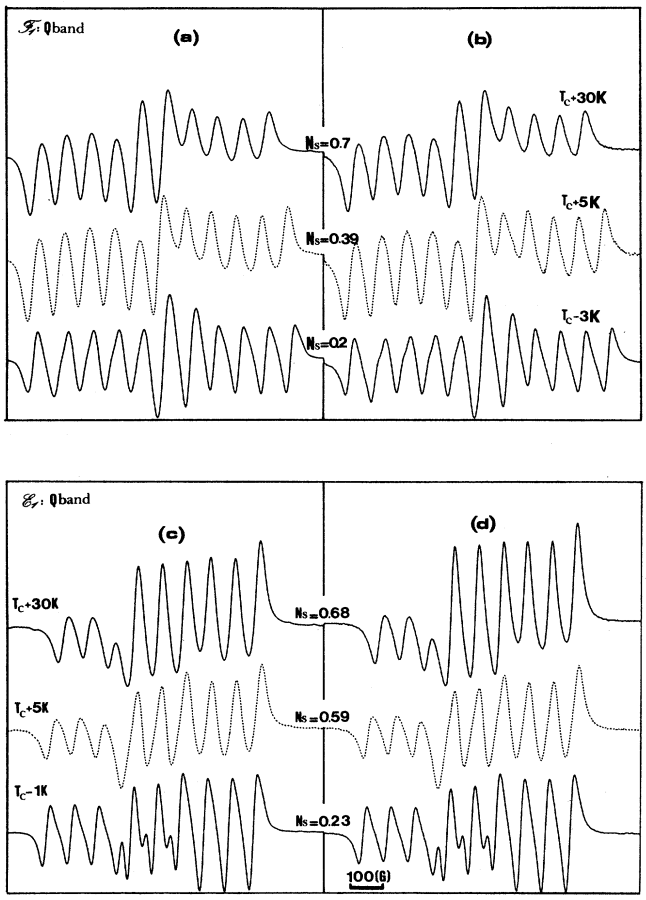

FIG. 3. Examples of simulations of the EPR spectras (in the Q band) for various temperatures using a convolution procedure. (b) The experimental $\mathcal{F}_1$ spectras and (a) the simulated ones. (d) The experimental $\mathcal{E}_1$ spectras and (c) the calculated ones.

pinned solitons ($N_s < 0.18$) and three discrete sextuplets corresponding to a normal spectrum from the commensurate phase. In Fig. 4 we have plotted $N_s = 0$ below $T_c - 5$ K.

III. DISCUSSION

A larger hysteresis $\Delta T = 10$ K than for samples grown from aqueous solution[11] is observed. This indicates that defects are present in our samples and this is consistent with dielectric measurements on samples of the same origin.[8] It is well known that the lock-in transition is very sensitive to defects and to the thermal history of the samples through a pinning effect.[8,12,13] Therefore, we cannot pretend to observe the intrinsic critical behavior of Rb_2ZnCl_4 near T_c.

On the other hand, we may question the relevance of the line-shape parameter $N_s(T)$ as an essential parameter monitoring the structural phase change. Let us note that two independent measurements on sample B, during the heating run, with the help of two different EPR transitions at the Q band, led to consistent results [Fig. 4(a)]. Moreover, at T_c, we obtain the same density of residual solitons of about $N_s(T_c) = 0.3$ whatever the samples, the ESR transition, and the measurements frequency. The consistency of these observations enforces the reliability of our estimate of the soliton density. Since the two samples are cleaved from different batches and since they have a different thermal history and since they are submitted to different thermal jumps, a different behavior near T_c is not surprising.

For the sample B, we obtained a continuous variation of $N_s(T)$ [Fig. 4(a)]. For comparison we have represented the intrinsic critical behavior according to $N_s(T) = -N_0 \ln^{-1}(t)$ with $N_0 = 1.89$, $t = (T - T_c)/T_c$, and $T_c = 194.9$ K. Searching for an exponent law, $N_s(T) \propto t^{\bar{\beta}}$, to fit the experimental result, we found that $\bar{\beta} = 0.3$. According to the theory,[12] a soliton regime dominated by defects should verify that $\bar{\beta} = 0.5$. Therefore, we cannot account for our results with the help of current theories. It is worth noting that the vanishing of $N_s(T)$ far below T_c is reached through a smooth tail [Figs. 4(a) and 4(b)] over a temperature range of 5 K below T_c. This indicates

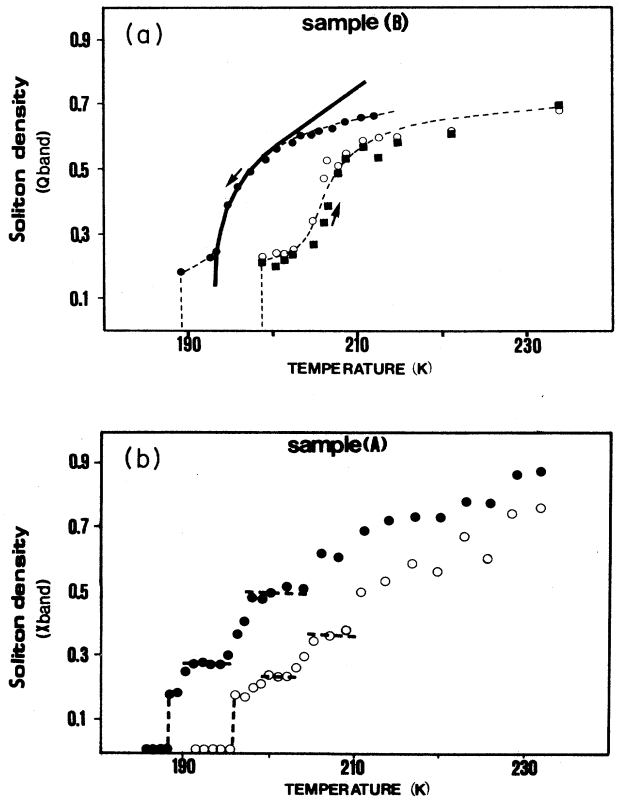

FIG. 4. The soliton density $N_s(T)$ deduced from the fitted parameter $\Delta(T)$: (a) Q-band measurements with sample (B): cooling (●) and heating run (○) for transition $\mathcal{E}_1$. Heating run (■) for transition $\mathcal{F}_1$. The solid line correspond to the theoretical law $N_s(T) = -1.89 \ln^{-1}[(T - T_c)/T_c]$. The dashed lines are guides for the eye. (b) X band for sample (A) and transition $\mathcal{E}_1$ cooling (●) and (○) heating.

a rearrangement of pinned solitons below and near T_c as it was also observed with the help of other techniques.[13]

The results obtained with the sample A are much more interesting. Indeed, the dependence of N_s on T is marked by several "plateaus" over temperature ranges of about 5 K. Due to the slow cooling and heating rates, these plateaus were observed for up to a few hours. In as much as our parameter $N_s(T)$ is a relevant one, we should have observed metastable states. Let us note that the conditions required for metastable states, i.e., the existence of pinning defects and smooth variation of T, were fulfilled for the sample A.

This result recalls a recent result obtained with $\{N(CH_3)_4\}_2$ $ZnCl_4$ using x-ray Bragg scattering.[14] In this crystal, defects were created by x-ray irradiation and their concentration was controlled by the exposure time and the thermal treatments were similar to ours. Metastable states were monitored by the stability, over a temperature range of about a few K, of the incommensurate wave vector of the Bragg satellitees. Different metastable states were observed for the cooling and heating runs, in accordance with our results. Presently, our local measurements cannot discriminate a chaotic organization of pinned solitons and a true long-range order between them. On the other hand, a rather long-range order is required to observe Bragg satellites. We conclude also that there is a complementarity of the two techniques for a full identification of the metastable states.

CONCLUSION

Despite the use of an impurity to monitor the soliton regime and rather heavy computer work, our preliminary results show that ESR is an interesting method for investigating the soliton regime, which is a field of current interest. A report about the dynamical parameters L_1 and L_2 [Eq. (2)], the origin of the phase parameters Φ_0^1, and the amplitude-modulation parameter τ will be given elsewhere. Let us note that the parameter τ, which was introduced to improve the fit of the experimental lines, could be an indirect evidence of amplitude solitons.

ACKNOWLEDGMENTS

One of us (K.A.) would like to thank Dr. G. Rius and Dr. B. Lamotte of le Centre d'Etudes Nucléaires de Grenoble (France) for their valuable help in the preliminary experiments on the EPR Q and S band. The Centre National de la Recherche Scientifique is affiliated with the Unité de Recherche Associée No. 807.

---

*Present address: Laboratoire de Spectroscopie du Solide, Faculté des Sciences, Université du Maine, route de Laval, 72017 Le Mans CEDEX, France.

[1]R. Blinc, I. P. Alexandrova, A. S. Chaves, F. Milia, V. Rutar, J. Seliger, B. Topic, and S. Zumer, J. Phys. C **15**, 547 (1982).

[2]I. P. Alexandrova, J. Mol. Struct. **83**, 403 (1982).

[3]M. Pezeril and J. C. Fayet, J. Phys. (Paris) Lett. **43**, L267 (1982).

[4]A. Kaziba and J. C. Fayet, J. Phys. (Paris) **47**, 239 (1986).

[5]A. Abragam, *The Principles of Nuclear Magnétism* (Oxford University Press, Oxford, 1961).

[6]A. Kaziba, M. Pezeril, J. Emergy, and J. C. Fayet, J. Phys. (Paris) Lett. **46**, L387 (1985).

[7]S. A. Jackson, P. A. Leep, and T. M. Rice, Phys. Rev. B **17**, 3611 (1978).

[8]G. Godefroy, B. Jannot, C. Dumas, and V. Janovec, Ferroelectrics (to be published).

[9]A. Leble and J. J. Rousseau (unpublished).

[10]J. Dolinsek and R. Blinc, J. Phys. C **21**, 705 (1988).

[11]K. Hamano, H. Sakata, K. Yoneda, K. Ema, and S. Mirotsu, Phase Trans. **11**, 279 (1988).

[12]T. Nattermann, J. Phys. C **16**, 4113 (1983).

[13]P. Prelovsek and R. Blinc, J. Phys. C **17**, 577 (1984).

[14]D. Durand and F. Denoyer, Phase Trans. **11**, 241 (1988).